Stem Cell Research 53 (2021) 102374

Contents lists available at ScienceDirect

Stem Cell Research

journal homepage: www.elsevier.com/locate/scr

Lab Resource: Multiple Cell Lines

Generation of three human induced pluripotent stem cell lines, LUMCi024-A, LUMCi025-A, and LUMCi026-A, from two patients with combined oxidative phosphorylation deficiency 8 and a related control

Ruben W.J. van Helden [a], Matthew J. Birket [a], Christian Freund [a,b], Christaan H. Arendzen [a,b], Harald M. Mikkers [b], Valeria Orlova [a], René I. de Coo [c,d], Christine L. Mummery [a,b], Milena Bellin [a,*]

[a] Department of Anatomy and Embryology, Leiden University Medical Center, Leiden, the Netherlands
[b] Leiden University Medical Center hiPSC Hotel, Leiden, the Netherlands
[c] Department of Neurology, Erasmus MC University Medical Centre, Rotterdam, the Netherlands
[d] Department of Toxicogenomics, Maastricht University, Maastricht, the Netherlands

A B S T R A C T

Combined Oxidative Phosphorylation Deficiency 8 (COXPD8) is an autosomal recessive disorder causing lethal childhood-onset hypertrophic cardiomyopathy. Homozygous or compound heterozygous mutations in the nuclear-encoded mitochondrial alanyl-tRNA synthetase 2 (*AARS2*) gene underly the pathology. We generated induced pluripotent stem cells (hiPSCs) from two patients carrying the heterozygous compound c.1774 C>T, c.2188 G>A and c.2872 C>T *AARS2* mutations, as well as a related healthy control carrying the c.2872 C>T *AARS2* mutation. All hiPSC-lines expressed pluripotency markers, maintained a normal karyotype, and differentiated towards the three germ layer derivatives *in vitro*. These lines can be used to model COXPD8 or mitochondrial dysfunction.

Resource Table

Unique stem cell lines identifier	1. LUMCi024-A (https://hpscreg.eu/cell-line/LUMCi024-A) 2. LUMCi025-A (https://hpscreg.eu/cell-line/LUMCi025-A) 3. LUMCi026-A (https://hpscreg.eu/cell-line/LUMCi026-A)
Alternative names of stem cell lines	1. LUMC0057iAARS03 2. LUMC0058iAARS01 3. LUMC0059iCTRL03
Institution	Leiden University Medical Center, LUMC
Contact information of distributor	Milena Bellin (m.bellin@lumc.nl) Ruben van Helden (r.w.j.van_helden@lumc.nl) Christian Freund (c.m.a.h.freund@lumc.nl)
Type of cell lines	iPSCs
Origin	Human
Cell Source	Skin Fibroblasts
Clonality	Clonal
Method of reprogramming	Replication-defective sendai virus, *OCT3/4, SOX2, KLF4* and *MYC*
Multiline rationale	Non-isogenic cell lines obtained from patients with three heterozygous compound mutations in the same gene (*AARS2*) and a related control with a single heterozygous mutation in the *AARS2*.
Gene modification	YES
Type of modification	De novo
Associated disease	Combined Oxidative Phosphorylation Deficiency 8 (OMIM: 614096)
Gene/locus	*AARS2* 6p21.1, NM_020745.4 Heterozygous *AARS2* c.1774 C>T and c.2188 G>A (LUMCi024-A, LUMCi025-A) Heterozygous *AARS2* c.2872 C>T (LUMCi024-A, LUMCi025-A, LUMCi026-A)
Method of modification	N/A
Name of transgene or resistance	N/A
Inducible/constitutive system	N/A
Date archived/stock date	

(*continued on next column*)

Resource Table (*continued*)

Unique stem cell lines identifier	1. LUMCi024-A (https://hpscreg.eu/cell-line/LUMCi024-A) 2. LUMCi025-A (https://hpscreg.eu/cell-line/LUMCi025-A) 3. LUMCi026-A (https://hpscreg.eu/cell-line/LUMCi026-A)

(*continued on next page*)

* Corresponding author.
E-mail address: m.bellin@lumc.nl (M. Bellin).

https://doi.org/10.1016/j.scr.2021.102374
Received 26 March 2021; Received in revised form 23 April 2021; Accepted 25 April 2021
Available online 29 April 2021

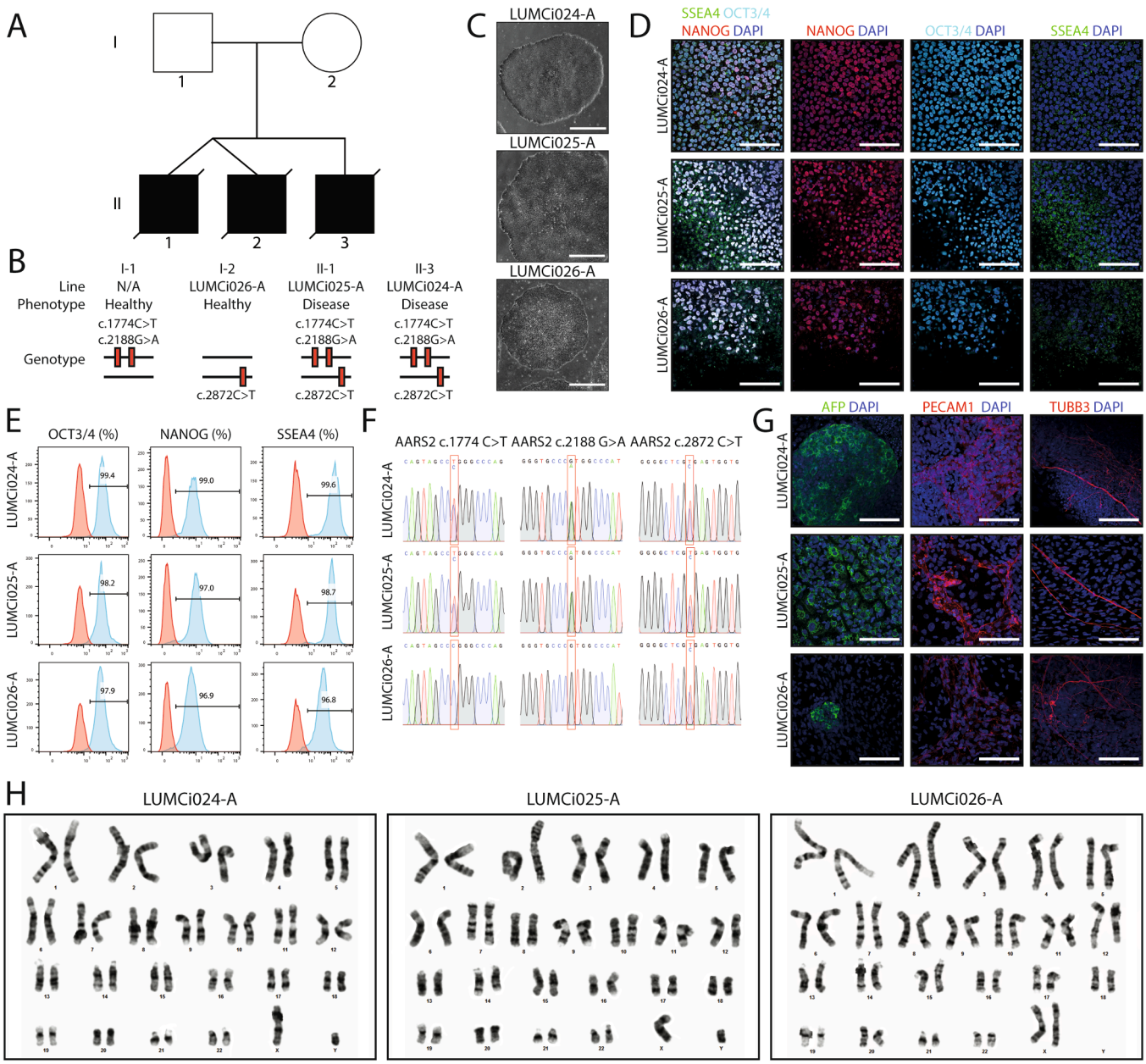

Fig. 1. Generation and characterization of hiPSC lines LUMCi024-A, LUMCi025-A and LUMCi026-A from patients affected by infantile cardiomyopathy due to mutations in the *AARS2* gene. (A) Family tree. (B) Schematic showing hiPSC lines with the corresponding genotypes. (C) Representative brightfield images showing hiPSC colony morphology. Scale bar: 600 μm (D) Immunofluorescence staining of iPSC colonies showing expression of the pluripotency markers NANOG (red), OCT3/4 (cyan) and SSEA4 (green) in all lines; nuclei stained with DAPI (blue). Scale bar: 100 μm. E) FACS analysis of undifferentiated hiPSCs stained for OCT3/4, NANOG and SSEA4. All lines show >95% marker expression versus unstained hiPSCs. (F) Sanger sequencing of genomic DNA isolated from hiPSC lines showing the presence of all three mutations (LUMCi024-A, LUMCi025-A) or only one mutation (LUMCi026-A). (G) Immunofluorescence staining of hiPSCs after spontaneous differentiation protocol for marlers of the three germ-layers, AFP (endoderm, green), PECAM1 (mesoderm, red), and TUBB3 (ectoderm, red). (H) Karyotyping of the three hiPSC lines showing no abnormalities.

Resource Table (*continued*)

Unique stem cell lines identifier	1. LUMCi024-A (https://hpscreg.eu/cell-line/LUMCi024-A) 2. LUMCi025-A (https://hpscreg.eu/cell-line/LUMCi025-A) 3. LUMCi026-A (https://hpscreg.eu/cell-line/LUMCi026-A)
Cell line repository/bank	August 2014 (LUMCi024-A & LUMCi025-A) September 2014 (LUMCi026-A) N/A
Ethical approval	Skin fibroblasts were collected after the patient (and children's parent) signed informed consent and

(*continued on next column*)

Resource Table (*continued*)

Unique stem cell lines identifier	1. LUMCi024-A (https://hpscreg.eu/cell-line/LUMCi024-A) 2. LUMCi025-A (https://hpscreg.eu/cell-line/LUMCi025-A) 3. LUMCi026-A (https://hpscreg.eu/cell-line/LUMCi026-A)
	approved by the ethical committee of the Erasmus MC University Medical Centre. The generation of the lines was approved by the Leiden University ethics committee under the P 13.080 "Parapluprotocol: hiPSC".

Table 1
Summary of lines.

iPSC line names	Abbreviation in figures	Gender	Age	Ethnicity	Genotype of locus	Disease
LUMCi024-A	LUMCi024-A	Male	Four days postnatal	Caucasian	Compound *AARS2* c.1774 C>T, c. 2188 G>A, c. 2872 C>T	COXPD8
LUMCi025-A	LUMCi025-A	Male	One day postnatal	Caucasian	Compound *AARS2* c.1774 C>T, c. 2188 G>A, c. 2872 C>T	COXPD8
LUMCi026-A	LUMCi026-A	Female	37	Caucasian	Heterozygous *AARS2* c.2872 C>T	Healthy

Table 2
Characterization and validation.

Classification	Test	Result	Data
Morphology	Brightfield microscopy	Normal morphology	Fig. 1 panel C
Phenotype	Qualitative analysis of IF staining	Positive immunostaining of pluripotency markers: SSEA4, OCT3/4 & NANOG	Fig. 1 panel D
	Quantitative analysis by FACS	Increased fluorescent signal over negative control of pluripotency markers: SSEA4, OCT3/4 & NANOG	Fig. 1 panel E
Genotype	G-band Karyotyping 5–10 Mb	Normal karyotype: 46, XY for LUMCi024-A and LUMCi025-A and XX for LUMCi026-A.	Fig. 1 panel H
Identity	Microsatellite PCR (mPCR) OR STR analysis	N/A 24 markers tested with 100% match	N/A Available with the authors
Mutation analysis	Sequencing	*AARS2* c.1774 C>T, c. 2188 G>A, c. 2872 C>T	Fig. 1 panel F
	Southern Blot OR WGS	N/A	N/A
Microbiology and virology	Sendai virus Mycoplasma	qPCR: Negative PCR analysis: Negative	Supplementary Fig. 1A Supplementary File 1
Differentiation potential	Spontaneous differentiation *in vitro* by IF analysis	Positive immunostaining of the three germ layer markers: ectodermal (TUBB3), mesodermal (PECAM-1) and endodermal (AFP)	Fig. 1 panel G
Donor screening (OPTIONAL)	N/A	N/A	N/A
Genotype additional info (OPTIONAL)	Blood group genotyping	N/A	N/A
	HLA tissue typing	N/A	N/A

1. Resource utility

These hiPSC lines are a valuable resource for studying COXPD8 and primary mitochondrial cardiomyopathies. Additionally, they can be used to study the cellular metabolism of human cardiomyocytes. These lines provide a unique tool to uncover the role of mitochondrial function in lethal infantile cardiomyopathy and to search for potential treatments (Table Resource Table).

2. Resource details

Combined Oxidative Phosphorylation Deficiency 8 (COXPD8) is a rare recessive familial disease characterized by mitochondrial dysfunction in the heart leading to fatal infantile hypertrophic cardiomyopathy (Götz et al., 2011). Part of a broader group of pathologies known as primary mitochondrial cardiomyopathies, COXPD8 is caused by mutations in the nuclear-encoded mitochondrial gene Alanyl tRNA-synthetase 2 (*AARS2*). The leading hypothesis is that mutations in *AARS2* cause instability in alanine-synthetase 2, leading to faulty loading of tRNAs in the mitochondria, defective assembly of mitochondrial-encoded oxidative phosphorylation chain proteins and impaired respiratory capacity (Euro et al., 2015; Sommerville et al., 2019). Due to the rare and lethal nature of this disease, primary tissue for research is rare. Human-induced pluripotent stem cells (hiPSCs) can be differentiated into patient-specific cardiomyocytes to uncover the mechanisms underlying this poorly understood pathology. Two patients with COXPD8 were identified just a few days after birth (Fig. 1A, Table 1). Sequencing of both the patients and their mother revealed the presence of three mutations in *AARS2* (Fig. 1B): the novel c.2872 C>T (p.958 R/*, rs779332260) mutation was present on the maternal allele; while in the patients, the paternal allele contained two mutations: the pathogenic c.1774 C>T (p.592 R/W, rs138119149) and the non-pathogenic c.2188 G>A (p.730 V/M, rs35623954) mutations. Dermal fibroblasts from all three donors were reprogramed using a replication-defective Sendai virus (SeV) containing the *OCT3/4, SOX2, KLF4* and *MYC* reprogramming factors (Nishimura et al., 2011). Three clones were isolated and expanded for each individual and cryopreserved at passage 5. One selected clone per line, hereafter named LUMCi024-A, LUMCi025-A, and LUMCi026-A, was assessed for *in vitro* pluripotency characteristics as reported in Table 2. All hiPSC lines showed characteristic stem cell colony-forming growth with a high nucleus/cytoplasm ratio (Fig. 1C). Expression and localization of pluripotency markers SSEA4, OCT3/4, and NANOG were verified using immunofluorescence (IF) analysis (Fig. 1D); fluorescence-activated cell sorting (FACS) confirmed expression of these proteins in the undifferentiated hiPSCs (Fig. 1E). Additionally, the absence of SeV was confirmed using qPCR for the SeV-NP DNA-vector in all lines (Supplementary Fig. 1A). Sanger sequencing showed all three patient mutations in LUMCi024-A and LUMCi025-A, and the presence of the c.2872C>T mutation in LUMCi026-A (Fig. 1F). Karyotype G-banding with a resolution of 5–10 Mb was used to confirm the genomic integrity of the hiPSC-lines, showing a normal karyotype and confirming gender (Fig. 1H). The differentiation potential of the lines was confirmed using an *in vitro* spontaneous differentiation assay with subsequent IF analysis for markers of the three germ layer derivatives, AFP (endoderm), PECAM1 (mesoderm), and TUBB3 (ectoderm) (Fig. 1G). To facilitate genotyping of all the lines and discrimination of the patient lines LUMCi024-A and LUMCi025-A, two primers were designed for an intronic region in the gene *MIF-AS1* which has a heterozygous SNP (g.117 T>G, rs2000466) in LUMCi025-A (Supplementary Fig. 1B). Finally, clones tested negative for the presence of mycoplasma (Supplementary file 1).

Table 3
Reagents details.

Antibodies used for immunocytochemistry/flow-cytometry			
	Antibody	Dilution	Company Cat # and RRID
Pluripotency Markers (FACS)	BV421 Mouse Anti-OCT3/4	1:25 (100 k cells in 80 ul)	BD Biosciences Cat# 565644, RRID: AB_2739320
Pluripotency Markers (FACS)	Mouse Anti-Human NANOG Monoclonal Antibody, PE Conjugated	1:5 (100 k cells in 80 ul)	BD Biosciences Cat# 560483, RRID: AB_1645522
Pluripotency Markers (FACS)	Anti-SSEA-4-FITC antibody	1:25 (100 k cells in 80 ul)	Miltenyi Biotec Cat# 130–098-371, RRID:AB_2653517
Pluripotency markers (Immunocytochemistry)	Mouse IgG2b anti-OCT3/4	1:100	Santa Cruz Biotechnology Cat# sc-5279 RRID: AB_628051
Pluripotency markers (Immunocytochemistry)	Mouse IgG1 anti-NANOG	1:150	Santa Cruz Biotechnology Cat# sc-293121 RRID: AB_2665475
Pluripotency markers (Immunocytochemistry)	Mouse IgG3 anti-SSEA4	1:30	BioLegend Cat# 330402, RRID: AB_1089208
Differentiation markers (Immunocytochemistry)	Mouse IgG2a anti-TUBB3	1:4000	Covance Cat# MMS-435P, RRID: AB_2313773
Differentiation markers (Immunocytochemistry)	Mouse IgG1 anti-CD31 (PECAM1)	1:100	Agilent Cat# M0823, RRID: AB_2114471
Differentiation markers (Immunocytochemistry)	Rabbit IgG anti-AFP	1:25	Quartett Cat# 2011200530, RRID: AB_2716839
Secondary antibodies (Immunocytochemistry)	Donkey anti-Mouse IgG (H + L) Highly cross-adsorbed Secondary, Alexa Fluor 488	1:500	Molecular Probes Cat# A-21206, RRID: AB_2535792
Secondary antibodies (Immunocytochemistry)	Donkey anti-Goat Mouse IgG (H + L) Highly cross-adsorbed Secondary, Alexa Fluor 647	1:500	Thermo Fisher Scientific Cat# A-11031, RRID:AB_144696
Secondary antibodies (Immunocytochemistry)	Goat anti-Mouse IgG3 Cross-adsorbed Secondary Antibody, Alexa Fluor 488	1:250	Thermo Fisher Scientific Cat# A-21151, RRID:AB_2535784
Secondary antibodies (Immunocytochemistry)	Goat anti-Mouse IgG1 Cross-adsorbed Secondary Antibody, Alexa Fluor 568	1:500	Thermo Fisher Scientific Cat# A-21124, RRID:AB_2535766
Secondary antibodies (Immunocytochemistry)	Goat anti-Mouse IgG2b Cross-adsorbed Secondary Antibody, Alexa Fluor 647	1:250	Thermo Fisher Scientific Cat# A-21242, RRID:AB_2535811
Primers			
	Target	**Forward/Reverse primer (5′-3′)**	
Mutation analysis (PCR/sequencing)	*AARS2* (c.1744 G>T)	GCCCACCACTAATAACCATTC/ TTCAGGATCCCACATCAGAG	
Mutation analysis (PCR/sequencing)	*AARS2* (c.2188 G>A)	GACTGCATGTTGGTCTTTCC/ ATAACCAGGTCCCCTACAGC	
Mutation analysis (PCR/sequencing)	*AARS2* (c.2872 C>T)	TTGAGGGTACCTTGAGTGGA/ TAGCCCATGTCTCCTTGTGT	
Genotyping (PCR/sequencing)	*MIF-AS1* (Intron 2 g.117 G>T)	TAGGCCTAGACCTTTCTCTC/ TCTTCCTAATCTTCACCCCA	
Sendai virus vector (RT-qPCR)	*SeV*	GCAGCTCTAACGTTGTCAAA/ CCTGGAGCAAATTCACCATGA	
Housekeeping gene (RT-qPCR)	*GAPDH*	TCCTCTGACTTCAACAGCGA/ GGGTCTTACTCCTTGGAGGC	

3. Materials and methods

3.1. Ethical statement

This study was approved by the Medical Ethical Committees at the Leiden University Medical Center (P13.080), the Erasmus Medical Center and the Maastricht University Medical Center. Written informed consent was obtained for all patients.

3.2. Cell culture and reprogramming

Skin fibroblasts were isolated from a skin biopsy and cultured in DMEM/F12 Glutamax supplemented with 10% FBS, 1% penicillin–streptomycin, 1% non-essential amino acids, 9 μM 2-mercaptoethanol and 1 μg/ml vitamin-C (all from ThermoFisher Scientific) at 37 °C, 5% CO_2 and 21% O_2. HiPSCs from skin fibroblasts were generated using Sendai virus with $1x10^5$ cells transduced once with 3–10 MOI SeVdp (KOSM302L). The day after transduction, cells were dissociated with TrypLE select and replated onto irradiated MEFs. The following day culture was continued in DMEM/F12 Glutamax supplemented with 20% KOSR, 10 ng/ml human FGF2, 1% non-essential amino acids, 0.5% penicillin–streptomycin and 0.1 μM 2-mercaptoethanol until the appearance of hiPSC clusters. Subsequently, cells were passaged once onto MEFs, and siRNA treatment for removal of SeV was initiated (Nishimura et al., 2011). Finally, colonies were picked and transferred onto Matrigel/mTESR at 37 °C, 5% CO_2 and 21% O_2 for expansion and stored at passage 5. Passaging was performed using Gentle Cell Dissociation Buffer (Stem Cell Technologies) by dissociating the cells into small clumps.

3.3. Immunofluorescence staining

HiPSCs at passage 10 were fixed in 2% PFA for 30 min, permeabilized with 0.1% Triton X-100, and blocked with 4% normal swine serum (NSS, DAKO) at room temperature (RT) for 1 h. Primary antibodies were added and incubated overnight at 4 °C. After washing, secondary antibodies were added for 1 h at RT (Table 3). Nuclei were stained with DAPI, and coverslips were mounted using Mowiol (Merck Millipore). Images were acquired on a Leica TCS SP8 microscope.

3.4. FACS staining

HiPSCs were dissociated at passage 15 with TrypLE for 5 min at 37 °C. Samples were fixed for 15 min in 200 μl of Reagent A of the fix & perm kit (Thermo Fisher Scientific). The cells were washed once in FACS buffer (PBS without Ca^{2+} and Mg^{2+} with 0.5% BSA and 2 mM EDTA), resuspended in 80 μl of Reagent B with the conjugated antibodies (table 3) and incubated in the dark for 60 min at RT. Subsequently, the samples were washed once and resuspended in FACS buffer before being measured on the MACSQuant VYB flow cytometer (Miltenyi Biotec).

Analysis was performed using the FlowJo^{tm} v.10.6.1.

3.5. In vitro spontaneous trilineage differentiation

The ability of hiPSCs to differentiate into the three germ layers (ectoderm, mesoderm, and endoderm) was assessed using a spontaneous differentiation protocol. The differentiated areas of the hiPSC colonies were picked and plated onto vitronectin-coated coverslips in TESR-E8 (Stem Cell). The next day the medium was refreshed with DMEM/F12 (Gibco) with 20% FBS (Gibco) and consecutively refreshed every second day. After three weeks of culture, the samples were fixed and stained as described.

3.6. qPCR

Total RNA from hiPSCs at passage 10 was extracted using the NucleoSpin® RNA kit (Macherey-Nagel). Following the manufacturer's instruction, reverse transcription was done on 1 μg RNA using iScript™ cDNA Synthesis Kit. qPCR was performed with primers, as shown in Table 3, using IQ SYBR Green Supermix and CFX96 Real-Time PCR Detection System (all from BioRad).

3.7. Karyotype analysis

HiPSCs at passage 9 were karyotyped by Cell Guidance systems (UK) and a total of 20 metaphases were counted.

3.8. Sequencing

Genomic DNA was isolated from hiPSCs using Quick Extract (Lucigen) according to the manufacturer's instructions. The *AARS2* gene was amplified at the three sites of the mutations using Platinum™ Taq DNA Polymerase High Fidelity (Invitrogen) for mutation analysis using the primers listed in Table 3. The PCR reaction was performed, and samples were submitted for Sanger Sequencing to confirm the presence of the *AARS2* mutations.

3.9. STR analysis

Cell identity was assessed on genomic DNA from both hiPSCs and corresponding skin fibroblasts by Promega PowerPlex Fusion System 5C autosomal STR kit (Westen et al., 2014).

3.10. Mycoplasma test

All lines were tested for the presence of mycoplasma and other human pathogens using the IDEXX BioAnalytics PCR analysis (Supplementary File 1).

Competing interests

Christine L. Mummery is co-founder of Pluriomics bv (now Ncardia bv).

Declaration of Competing Interest

The authors declare that they have no known competing financial interests or personal relationships that could have appeared to influence the work reported in this paper.

Acknowledgements

We thank Dr. M. Nakanishi (National Institute of Advanced Industrial Science and Technology, Japan) for providing SeV, P. de Knjiff (Dept. of Human Genetics, Leiden University Medical Center, NL) for STR analysis, and Dr. A.J.T.M. Helderman – van den Enden (Maastricht University, NL) for recruiting the patients. This work was supported by the European Research Council (ERCAdG 323182 STEMCARDIOVASC); the Netherlands Organization for Health Research and Development ZonMW (MKMD project no. 114022504); The Netherlands Organ-on-Chip Initiative, an NWO Gravitation project funded by the Ministry of Education, Culture and Science of the government of the Netherlands (024.003.001). RdC supported by NeMO foundation.

Appendix A. Supplementary data

Supplementary data to this article can be found online at https://doi.org/10.1016/j.scr.2021.102374.

References

Euro, L., Konovalova, S., Asin-Cayuela, J., Tulinius, M., Griffin, H., Horvath, R., Taylor, R.W., Chinnery, P.F., Schara, U., Thorburn, D.R., Suomalainen, A., Chihade, J., Tyynismaa, H., 2015. Structural modeling of tissue-specific mitochondrial alanyl-tRNA synthetase (AARS2) defects predicts differential effects on aminoacylation. Front. Genet. 5, 1–12. https://doi.org/10.3389/fgene.2015.00021.

Götz, A., Tyynismaa, H., Euro, L., Ellonen, P., Hyötyläinen, T., Ojala, T., Hämäläinen, R., Tommiska, J., Raivio, T., Oresic, M., Karikoski, R., Tammela, O., Simola, K.J., Paetau, A., Tyni, T., Suomalainen, A., 2011. Exome sequencing identifies mitochondrial alanyl-tRNA synthetase mutations in infantile mitochondrial cardiomyopathy. Am. J. Hum. Genet. 88 (5), 635–642. https://doi.org/10.1016/j.ajhg.2011.04.006.

Nishimura, K., Sano, M., Ohtaka, M., Furuta, B., Umemura, Y., Nakajima, Y., Ikehara, Y., Kobayashi, T., Segawa, H., Takayasu, S., Sato, H., Motomura, K., Uchida, E., Kanayasu-Toyoda, T., Asashima, M., Nakauchi, H., Yamaguchi, T., Nakanishi, M., 2011. Development of defective and persistent Sendai virus vector: a unique gene delivery/expression system ideal for cell reprogramming. J. Biol. Chem. 286 (6), 4760–4771. https://doi.org/10.1074/jbc.M110.183780.

Sommerville, E.W., Zhou, X.-L., Oláhová, M., Jenkins, J., Euro, L., Konovalova, S., Hilander, T., Pyle, A., He, L., Habeebu, S., Saunders, C., Kelsey, A., Morris, A.A.M., McFarland, R., Suomalainen, A., Gorman, G.S., Wang, E.-D., Thiffault, I., Tyynismaa, H., Taylor, R.W., 2019. Instability of the mitochondrial alanyl-tRNA synthetase underlies fatal infantile-onset cardiomyopathy. Hum. Mol. Genet. 28, 258–268. https://doi.org/10.1093/hmg/ddy294.

Westen, A.A., Kraaijenbrink, T., Robles de Medina, E.A., Harteveld, J., Willemse, P., Zuniga, S.B., van der Gaag, K.J., Weiler, N.E.C., Warnaar, J., Kayser, M., Sijen, T., de Knijff, P., 2014. Comparing six commercial autosomal STR kits in a large Dutch population sample. Forensic Sci. Int. Genet. 10, 55–63. https://doi.org/10.1016/j.fsigen.2014.01.008.